



## Glucomannan for Food Packaging Biofilms: Faceting of the Polymer Film

---

Kholoud Al-Ajlouni, Paul D. Fleming and  
Alexandra Pekarovicova

EasyChair preprints are intended for rapid  
dissemination of research results and are  
integrated with the rest of EasyChair.

July 22, 2021

# Glucomannan for food packaging biofilms: Faceting of the polymer film

*Kholoud Al-Ajlouni<sup>1</sup>, Paul D. Fleming<sup>1</sup>, Alexandra Pekarovicova<sup>1</sup>.*

<sup>1</sup> Chemical and Paper Engineering, Western Michigan University- USA.

E-mail: [kholoudsaleh.alajlouni@wmich.edu](mailto:kholoudsaleh.alajlouni@wmich.edu), [dan.fleming@wmich.edu](mailto:dan.fleming@wmich.edu), [a.pekarovicova@wmich.edu](mailto:a.pekarovicova@wmich.edu).

## Short Abstract.

Glucomannan, a natural hemicellulose that comes from the roots of a plant called Konjac, is a promising material for food packaging and printed electronics films. Unlike petroleum-based films, glucomannan films are biodegradable, safe, and eco-friendly. Glucomannan films should be transparent, clear, create water vapor and oxygen barrier and have good mechanical properties. In this work, the films were formulated from three constituents: glucomannan, surfactant and a plasticizer. Mixing the ingredients was done at a constant temperature at 35°C and 6000 rpm. Upon drying in an Environmental Chamber (50°C and 11.4% RH and 18-36 hours); after 3 hours, the films, showed shape transformation and surfactant freezing and depositing on the glucomannan-water interface. This deformation structure had shapes that looked like polygons and long fibers. This is faceting of the droplets of glucomannan gel solution during the slow cooling process or so called interfacial freezing phenomena. Faceting of the glucomannan gel droplets reduced the film's clarity, strength, and vapor's permeability, these deformed films are not suitable for packaging nor for printed electronics. We found that for a successful film formation, controlling the reaction temperature of the components at 40°C and the drying conditions in an Environmental chamber (57°C and 35% RH) is necessary.

**Keywords:** Glucomannan, Faceting, Transparent, Stretch wrapping biofilms, Packaging, Surfynol 104H.

## 1. Introduction and background

Wrapping films used in packaging of food, electronics, or other items are stretch elastic films that keep items firmly bound during storage or transportation. Commonly, they are made from linear low-density polyethylene (LLDPE) or other petroleum-based chemicals. Biofilms are synthesized from natural biomasses; they are eco-friendly, biodegradable, and they degrade naturally and faster (Rhim and Ng, 2007), (Honarvar, Hadian and Mashayekh, 2016). One of possible materials to create these biofilms is glucomannan. Glucomannan is a hemicellulose mainly extracted from the roots of Konjac or elephant yam plant; it is a hetero polysaccharide which contains different saccharides, such as mannose and glucose. Its backbone consists of linked  $\beta$ -D-1 $\rightarrow$ 4-D-manopyranose and D-glucose, which are often acetylated (Scheller and Ulvskov, 2010) as shown in Figure 1.

Packaging films from hemicelluloses are safe, inexpensive and considered as oxygen barriers; however, they lack proper mechanical and water barrier properties (Jonas, 2006). To reinforce the strength, composite films from glucomannan and polymers such as cellulose (Kalia *et al.*, 2011), micro or Nano-fibrillated cellulose NFC (Lavoine, Desloges and Bras, 2014), (Ma, Pekarovicova and Fleming, 2018), or different hemicelluloses (Wang *et al.*, 2017) , (Nair, Alummoottil and Moothandasserry , 2017) are added.

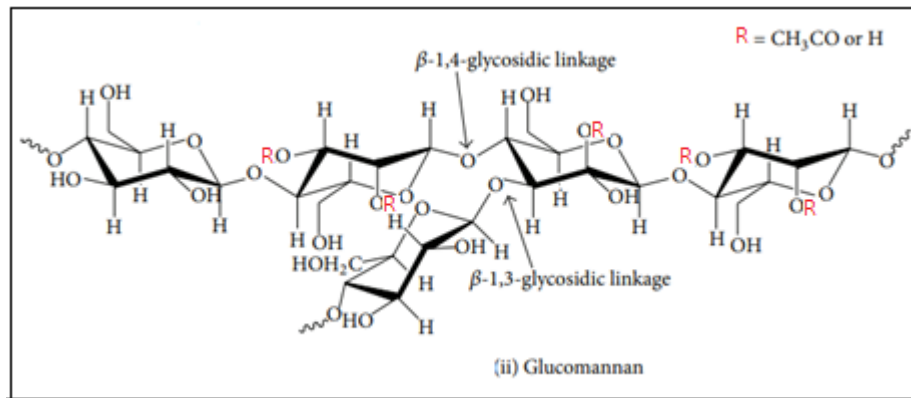


Figure 1. The chemical structure of glucomannan (Lee, Hamid and Zain, 2014).

For packaging purposes, the rheology of the polymers influences the production and control processes because they behave as liquids and solids at the same time, as called viscoelastic (Triantafillopoulos,1988). Printing labels on packaging films require smooth surfaces and free from 3D structures. Those requirements apply also for printed electronics (Ma, 2018).

Films were formulated from a polymer, surfactant, and plasticizer at 35°C, then they must be casted and dried. Drying is an important step of the process, slow cooling of the formed gel could stimulate the transformation of polymer droplets in surfactant solutions into deformed solid shapes. In general, as the temperature is decreased, the droplets of the polymer-surfactant solution in water will undergo changes from spheres into polyhedra (Wong *et al.*, 2019), (Marin *et al.*, 2020), platelets and finally platelets with a tail (Guttman *et al.*, 2016) (García-Aguilar *et al.*, 2021), (Denkov *et al.*, 2015). The interface of these deformed droplets had a frozen solid monolayer, once it is formed, it will not be further changed.

The market for bio-based film packaging is growing very fast because the need for biodegradable and sustainable films for packaging is globally recognized. Governments encourage companies to produce non- fossil- based packaging materials by tax exemption of the raw materials and trade regulations. Cellulose based films market is segmented into wrapping films, bags, labels, tapes and others. Several financial reports say that in 2007, the revenue of the packaging from cellulose films was \$ 629.8 M and predicting to expand more at a compound annual growth rate of 4.9% in the period 2018 to 2028, Figure 2.

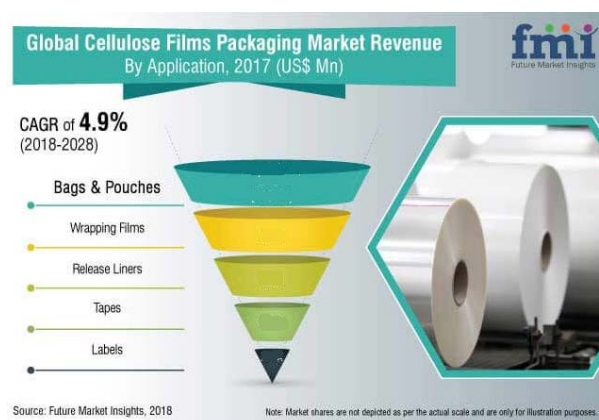


Figure 2. Worldwide Market of Cellulose film Packaging in 2017, Based on application (Cellulose Film Packaging Market - Global Industry Analysis, Size and Forecast, 2018 to 2028, 2021).

Countries covered by this market are North America and Europe, which constitute over 40.4% of the global market in 2018, South Asia, Middle East, Africa and some countries in South America. Examples of the packaging companies are: Bemis Company, Crown Holdings, Reynolds, Celanese corporation, Futamura Chemical Co., Eastman Chemical Company, Sappi limited and others (Cellulose Film Packaging Market - Global Industry Analysis, Size and Forecast, 2018 to 2028, 2021). One kilogram of cellulose film ranges from US\$ 3.75-4.5 produced by Hubei Golden Ring New Material Tech Co. Ltd, from China, and US\$ 0.05 per meter by Masmak Kateryna Piasecka From Poland (Alibab.com). Up to our knowledge films from hemicellulose, such as Glucomannan or xylan or composite films are still not commercially produced mainly because cellulose based films are stronger and have good barrier properties.

## **2. Materials and Methods**

### **2.1 Materials**

Glucomannan from NOW Food Company; Sorbitol from Alfa Desar; Surfynol 104 PA from Air Products and Chemical Inc., and deionized water were used.

In this batch of experiments, a casting method was followed. The dose of the non-ionic Surfynol 104PA surfactant varied from 0% to 40% of the glucomannan on mass basis.

### **2.2 Film formation procedures:**

1. In a 500 ml beaker, glucomannan was dissolved in 100 ml of deionized, DI, water at room temperature, the beaker was placed in a water bath at 35 °C. A rotary mixer at a speed 6000 rpm was used to mix the solution for 15 minutes. The top of the beaker was covered to prevent evaporation of water.
2. Surfynol 104PA was added to the solution, according to Table 1, and mixed for 3 minutes, and finally Sorbitol was added and mixed for 3 more minutes.
3. For rheology testing, contact angles, surface tensions, samples of 5-10 ml of the gel solution were taken and kept in the water bath until testing. The rest of the gel solution was poured into a previously washed Petri dish by ethylene glycol, and then dried in an Environmental Testing Chamber at 50°C and 11.4% Relative Humidity (RH) for 3 hours.
4. The temperature was then changed to TAPPI conditions of 23°C and 50 % RH for the rest of average drying time, 18- 36 hours.
5. The film was peeled off and stored in a plastic bag before testing.
6. Some selected properties were measured, rheological, surface free energies, mechanical and barrier properties.

Table 1: Glucomannan film's formulations.

Film	Glucomannan [g]	Surfynol 104 H [g]	Sorbitol [g]
1	1	0.1	0.2
5	1	0.2	0.2
13	1	0.4	0.2
15	1	0	0.2
16	1	0.05	0.2

### 2.3 Density measurement.

Density is the first property to be measured for the gels and is needed for calculating the contact angle and the surface free energy; its value is plugged into the software of FTA 200 each time the concentration of the surfynol was changed. Gardco stainless steel cups are metallic pycnometers having the exact volume of 8.32 ml at 20°C. The cup is weighed, with and without the samples, and the density is calculated by dividing the mass difference (g) by 8.32 ml.

### 2.4 Rheological measurements

An Anton Paar instrument was used. The solution fills a 1 mm gap between two plates, and the rotational speed is selected to produce a shear rate, the rheometer determines the necessary shear stress to deform the gel. Viscosity is determined by the software as the quotient of shear stress and shear rate, different rheogram curves can be produced to illustrate the relation between rheology parameters. The dynamic viscoelastic measurements of the glucomannan solutions were also carried out by The Anton Paar. The storage and loss shear moduli,  $G'$  and  $G''$ , were measured under frequency sweep test, 0.1-628 Hz. The overall rigidity of the solutions is the sum of both moduli. If the storage modulus  $G'$  is higher than the loss modulus  $G''$ , this means that the solution is more elastic than viscous, and vice versa. The relation between the two moduli is that  $\tan \delta = G''/G'$  which is a quick way to identify the overall behavior of the gel, if  $\tan \delta < 1$  then the gel is more elastic than viscous. (*Rheological measurements* :: Anton Paar Wiki, no date).

### 2.5 Surface tension and contact angles

Surface tension can be measured using the FTA 200 instrument, by the pendant drop analysis. A drop of the gel falls over a glass slide by a controlled needle pump, a camera captures 310 images of the falling drop and the software recorded it. The contact angle is selected from the images where the drop touches the surface of the substrate and has the shape of axisymmetric menisci and then calculated using the Young equation. The surface tension image is selected when the droplet is about to separate from the tip of the needle and land on the substrate (Chau, 2009).

### 2.6 Caliper of the Glucomannan films.

Caliper or thickness of the dry films is measured by automated Technidyne Profile plus instrument. The accuracy is  $\pm 0.508$  micro meter. The thickness of the film is important in

determining the permeability and for tensile tests of the films

## 2.7 Mechanical properties

Tensile strength, yield strain, and % elongation of the films defines the ability of the packaging films to stretching and ensuring a good seal. Packaging products, such as packing tape, are preferred to have higher tensile strength so that they can keep the products sealed and secured during shipping; stretching films also provide protection from damage. Samples of 100 cm by 15 cm were gripped in an Instron 430I and pulled apart, 500 N load and 2.5 cm/min speed, until it breaks. Software in a computer attached to the Instron, will give the values of tensile strength and % elongation, among other properties, during the process until it reaches the break point.

## 2.8 Barrier property

Packaging films should keep moisture and aroma inside food and packed materials, making a barrier from losing them is essential for both consumers and producers. The ability of a film to pass air and moisture through films defines air and water vapor permeability, testing films usually follow TAPPI standard methods. Permeability depends mainly on the porosity and thickness of the films and the fluid's pressure drop, which was first derived by Darcy's equation in the 19<sup>th</sup> century, it describes the transport of fluids through porous material. According to TAPPI T-555, Messmer Instrument Parker Print Surf measures the PPS porosity of the films and Air permeability coefficient K is calculated from a relation proposed by Pal et., el.  $K(\text{um}) = 0.48838 * Q (\text{ml/min}) * L(\text{m})$  (Pal, Joyce and Fleming, 2006). However, permeability of water vapor can be tested by ASTM E96 using Thawing-Albert EZ- cup". Air permeability is a measure of barrier property of vapor and moisture inside the materials, if air cannot escape out of the packaging film, nor will gases or water vapors.

## 2.9 Transparency

Food packaging should be clear and transparent therefore it shows what inside it. The transparency is measured by the total transmittance, it depends on the type of polymer, and the thickness of the film. A SpectroScan Automated Scanner 36.62.11 was used to measure the transparency of the films.

## 3. Results and discussion

Characterization of biofilms is important to identify the polymers and their performances in food packaging and in printed electronics. Rheology parameters such as shear rate, shear stress and viscosity, have their influence on film's production and quality control processes (Picout and Ross-Murphy, 2003). They give a perception of the ease of flow of the polymeric films during film making and other flow dependent properties.

The formulation of glucomannan films was done using three components: glucomannan, surfactant Surfynol 104H and sorbitol as a plasticizer. Previous researches, selected the reaction temperature of the polymer with other components as 45°C (Ma, Pekarovicova and Fleming, 2018) or 60°C (Wang *et al.*, 2017) in the production of glucomannan films. In this work, we selected a lower temperature of 35°C to reduce the energy consumption in industry. Upon casting, the glucomannan solution was like a gel, clear and homogenized but after cooling, the final dried film was distorted with solid structures, faceted, and grew tails, similar

to those in Figure 3. The cooling rate of the films is affected by temperature, relative humidity, type of and concentration of the surfactant used. The surfactant reduced the surface tension of the solution and made evaporation of water faster, however, increasing the surfactant reached a value where its surface tension remained constant (Kajiya *et al.*, 2009). To understand what caused the faceting of the glucomannan gel, we studied the effect of the surfactant concentration on the stability of the films when reacting at 35°C and undergoing a cooling process of 50°C and 11.4% RH.

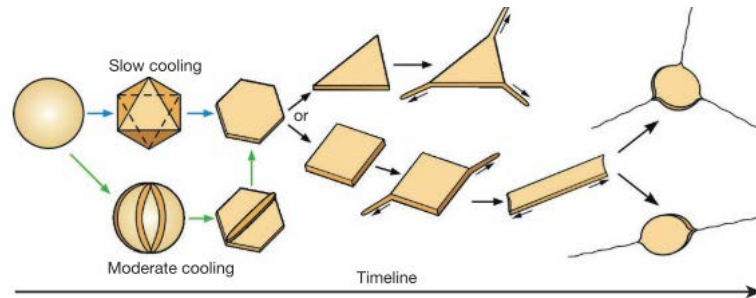


Figure 3: The timeline of shape transformations of an oil-droplet emulsion (Denkov *et al.*, 2015)

### 3.1 Density

The density of the gels of glucomannan was measured, Table 2. The density, is almost the same, the addition of the surfactant didn't change significantly the value of the density as expected; for example, the calculated value of the density, given by the calculator for Gluc. 0.2 g is 1.00581721 and for Gluc. 0.4 is 1.00466, but when rounding to 3 significant digits (the fewest significant number of the volume 8.32) the values become 1.00 and 1.01 g/cm<sup>3</sup> respectively.

### 3.2 Rheology of the polymers.

Biopolymers such as glucomannan are considered as viscoelastic materials, and they behave as Non-Newtonian shear-thinning solutions. When the viscosity is measured by the Anton Paar Rheometer, parallel plates were used in the measuring system (*Rheological measurements :: Anton Paar Wiki*, no date). The viscous behavior of Glucomannan gels had been tested using Anton Paar, Figure 4 represents the viscosity against the shear rate for the faceted glucomannan gels. It is shown that the viscosity decreased as the shear rate increased, which indicates that these gels had a shear-thinning behavior, and the viscosity also decreased when the concentration of the surfactant increased. The surfactant Surfynol 104 H is a non-ionic surfactant, 25% Ethylene glycol; when absorbed at the air-water interface, the hydrophobic parts of the surfactant are aligned in air, thus breaking the interactions between water molecules, and thus reducing the surface tension which explains the reduction of the inner resistance to flow and thus lowering of the viscosity values. From the curves, the gel of viscosity of 0.1 g surfactant deviated from the trend of reduction of viscosity.

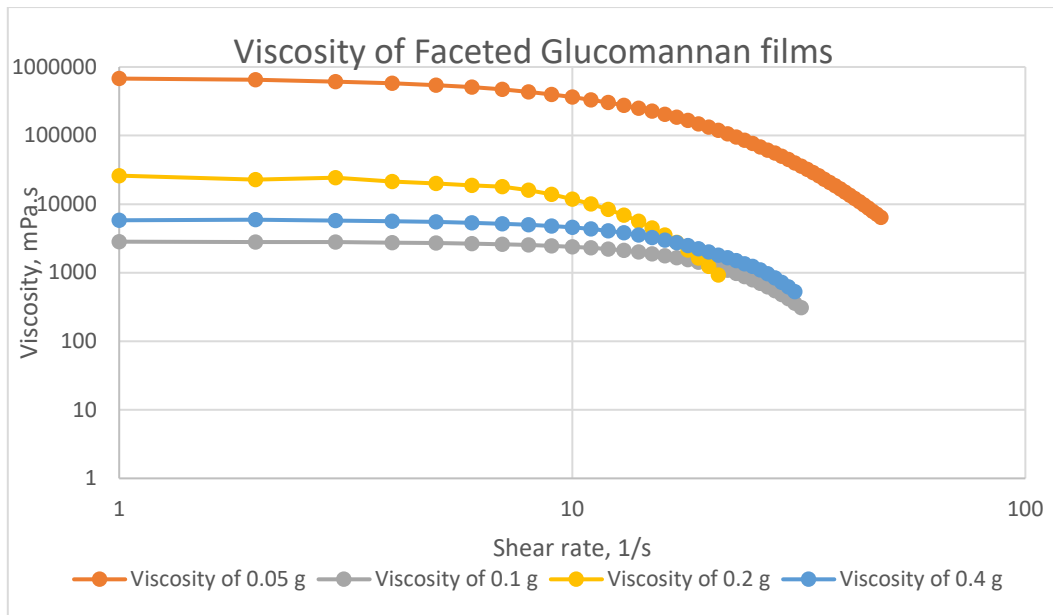


Figure 4: The viscosity and shear rate relationship for different glucomannan gels.

The viscoelastic behavior of the gel solutions of glucomannan showed that they behave as liquids at small angular frequencies and their  $\delta d < 1$ , but they become elastic at higher frequencies. All of the glucomannan with surfactants gels experienced a turning point from viscous to elastic behavior at frequency  $\sim 7.5$  rad/s, whereas the gel without surfactant became elastic at angular frequency  $\sim 0.13$  rad/s. Figure 5 shows how the storage modulus  $G'$  and the loss modulus  $G''$  depend on the angular frequency and the dual ability of the gels to act like liquids and solids as frequency changes.

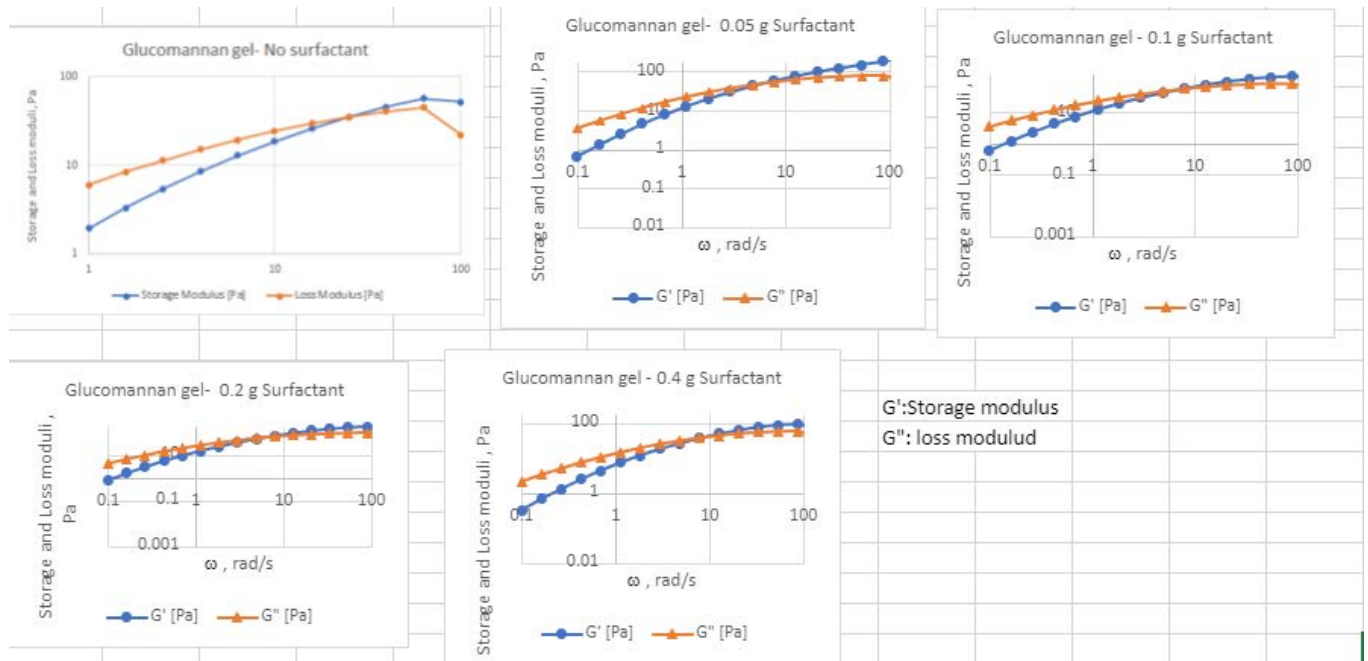


Figure 5: Frequency sweep for different glucomannan gels.

### 3.3 Surface tension.

The surface tension of the gel is an important property in printing applications, also the contact angle is vital in determining the surface free energy of substrates, and wetting properties of printed inks. The surface energy of the substrate should be higher than that of the ink to assure good spreading of the ink during the printing process. Surfactants have hydrophilic and hydrophobic parts, which when becoming in contact with polymer, both hydrophobic parts make strong bonds causing the reduction of the solution surface tension, this allows the dissolution of the polymer in water; this gives the chance of other polymers or chemicals to react and produce a complex network that will improve the mechanical and thermal properties of the main polymer. The values of surface tension of glucomannan gels are illustrated in Table 2.

*Table 2: Contact angle and surface tension of the glucomannan gels.*

Surfactant concentration, [w/w %]	Density, [g/cm <sup>3</sup> ]	Contact angle over glass, [degree]	St dev	Surface tension, [mN/m]	St dev
0	1	43.09	0.47	38.17	5.21
5	1	72.64	3.75	24.45	0.36
10	1	57.29	0.14	22.28	0.16
20	1.01	44.55	1.73	22.15	0.80
40	1	42.13	0.62	19.6	0.55

Figure 6 demonstrates pendant droplets of the glucomannan solutions, from the images captured by FTA 200. The surface tension of each was calculated from the shape of the pendant droplet.

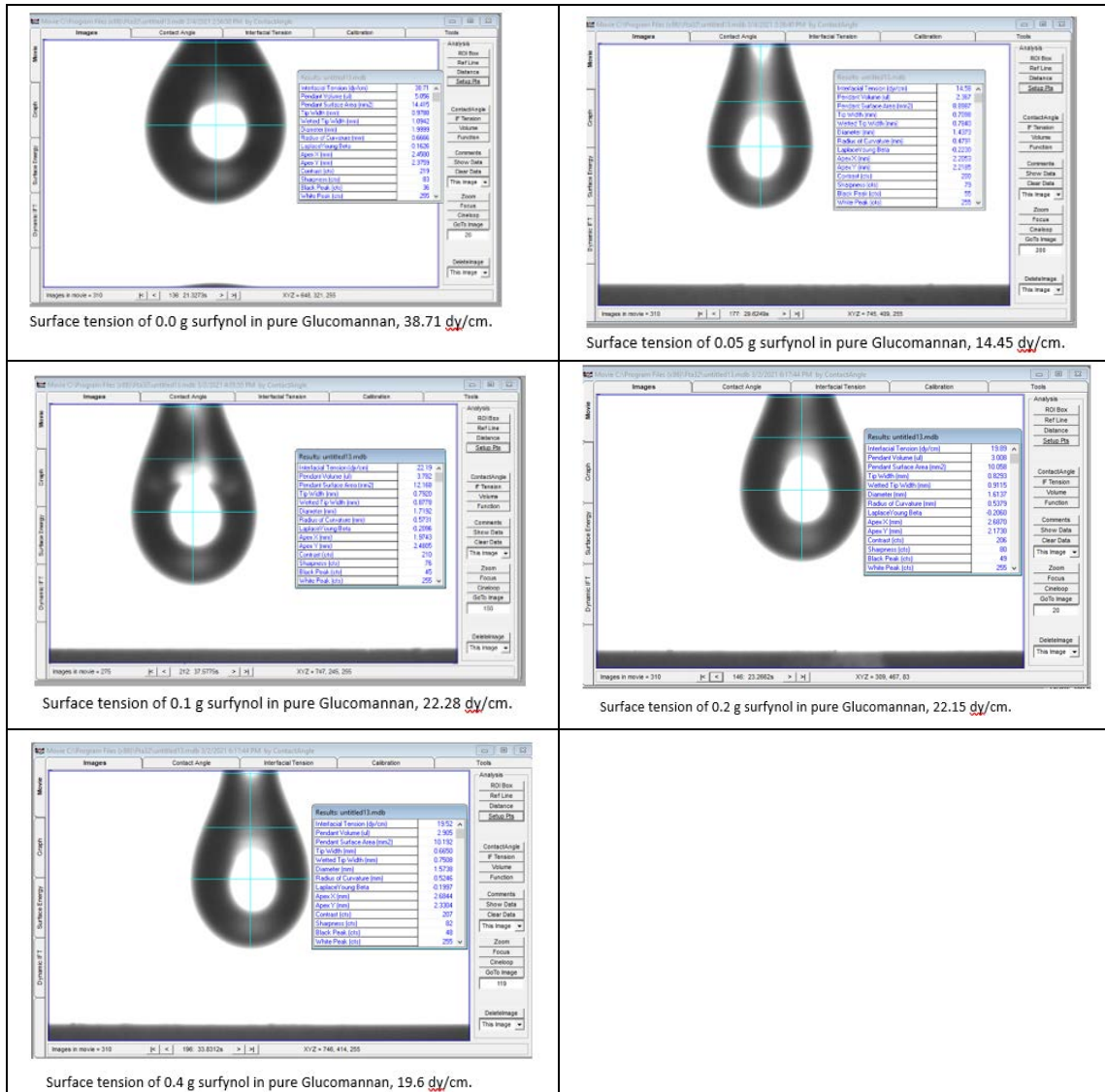
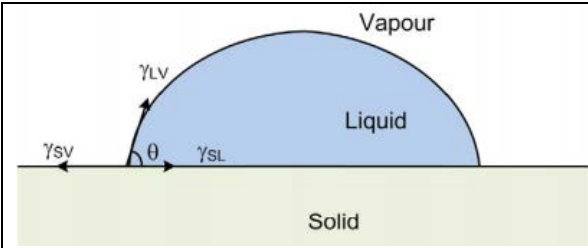


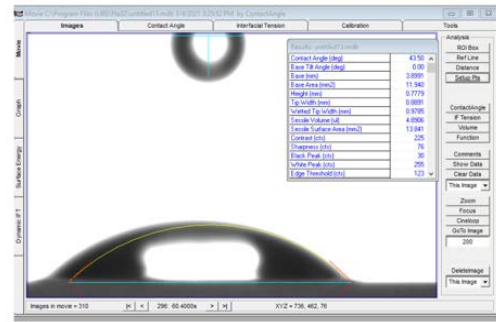
Figure 6: The surface tension of glucomannan solutions [mN/m] at different surfactant concentrations, (g surfactant/g glucomannan)

### 3.4 Contact angles.

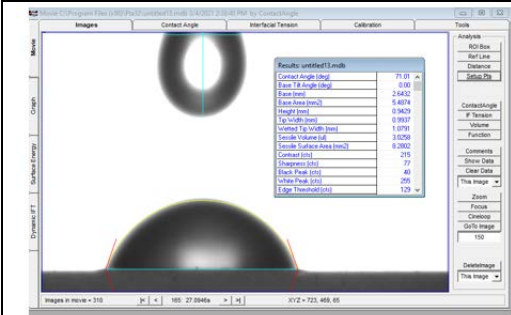
Contact angle can be used to characterize the surface wettability and the surface energy of the glucomannan solutions by using Young's equation:  $\gamma_{SV} = \gamma_{SV} + \gamma_{LV} \cos \theta$  (Makkonen, 2016), Owens-Wendt (1969) (Owens and Wendt, 1969) or AMF equations (Altay *et al.*, 2020). The classical view of the contact angle demonstrates where the force balance at the contact line between the 3 phases. The AMF method measures the surface tension of the liquid and the contact angle from the images of FTA 200 and then calculates the surface energy of the solid surface introducing a new parameter,  $\alpha$ , that satisfies the inequality  $\gamma_{SV} + \gamma_{SL} - \gamma_{LV} > 0$ , where  $\gamma_{SV} = \frac{\gamma_{LV} \cos^2(\theta/2)}{\alpha}$  (Altay *et al.*, 2020). The contact angles in Table 2 show that the gel drops spread greater when more surfactant is added. The surface tension of the drops of the glucomannan solution are illustrated in Figure 7, it is also the same tendency of the contact angles. This behavior is vital in smooth printing of the glucomannan solution over a board in printed electronics and on printing labels on food packaging films.



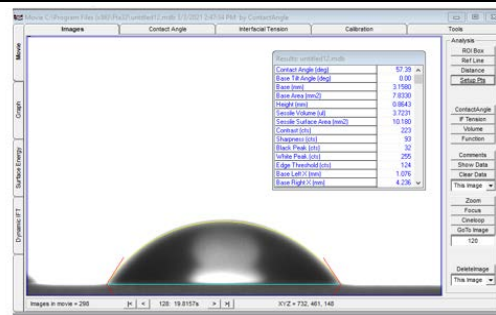
Force balance at the contact line between the solid surface and the liquid and air. The surface tensions between each 2 phases are in equilibrium (Makkonen, 2016).



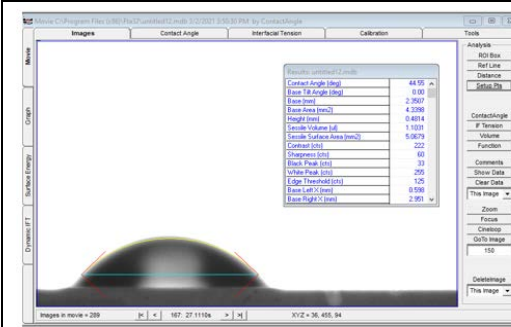
Contact angle of 0.0 g surfactant in pure Glucomannan, 43.09°.



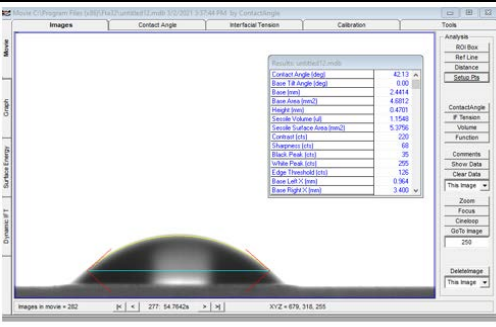
Contact angle of 0.05 g surfactant in pure Glucomannan, 72.64°



Contact angle of 0.1 g surfactant in pure Glucomannan, 57.29°.



Contact angle of 0.2 g surfactant in pure Glucomannan, 44.55°.



Contact angle of 0.4 g surfactant in pure Glucomannan, 42.13°.

Figure 7: The contact angle of glucomannan gels over glass at different surfactant concentrations (g surfactant/ g glucomannan) from FTA 200 and contact angle theory demonstration (Makkonen, 2016).

### 3.5 Caliper of the Glucomannan films.

The thickness, caliper, of the films depends mainly on casting and drying conditions of the films. Faceted areas were thicker and hard, which made it difficult to stretch and easier to break. Figure 8 illustrates the different calipers of the biofilms and the petroleum-based film, polyethylene film.

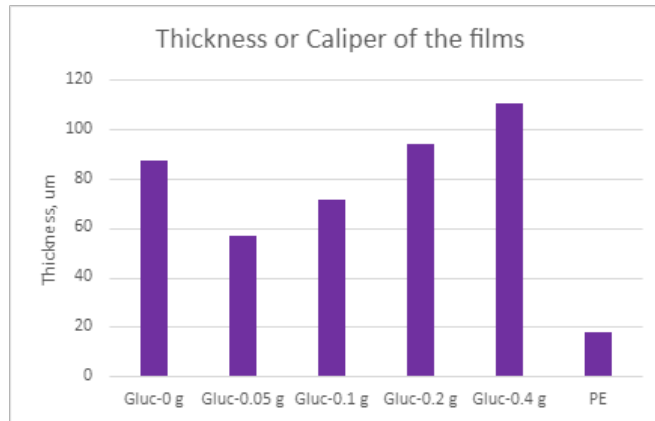


Figure 8: The thickness of glucomannan films compared with the polyethylene.

### 3.6 Tensile strength and elongation of the films.

Tensile strength and elongation of the films were measured as a result of applying 500 N force on both ends of stripes of the films, 10 cm  $\times$  1.5 cm until breaking point. The thickness of the films was not homogenized in each faceted film and affected the tensile strength at break of the films, the thinnest films showed more resistance to tensile stress. Elongation was also in the same pattern; more stretching was notable in thin films. Figure 9 shows the three relations together, it shows a comparison of the faceted films and a Polyethylene PE cling wrap from Glad company. The PE wrap film elongation was 7 folds of the highest elongation Glucomannan films had, Gluc. 0.05, but the tensile strength at break was weaker.

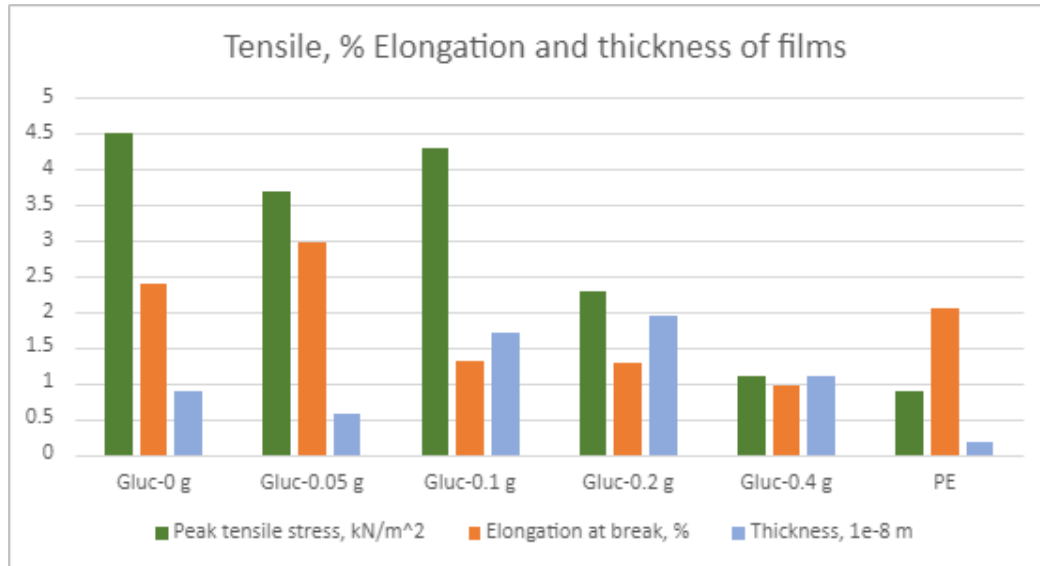


Figure 9: Tensile strength, % elongation of the films at break and the thickness of the glucomannan films, the % elongation of the PE is 20%, but plotted as  $1\text{e-}2$  of the value for comparison purposes.

### 3.7 Barrier properties

Air, gas, and vapor permeability is not favored in food packaging world as mention earlier, it should be at its minimum values. Following Pal et., el. Team to calculate air permeability, the thickness and the PPS porosity should be measured first and then the air permeability can be

calculated according to their equation. Figure 10 illustrates the porosity of the faceted films as well as PE film, the polyethylene film has the lowest permeability since it is the thinnest film and lower permeability coefficient. Between the faceted films the film of 0.05 g surfactant had low PPS porosity and caliper, which explains its tendency to be air-flow resistance and water vapor as a result.

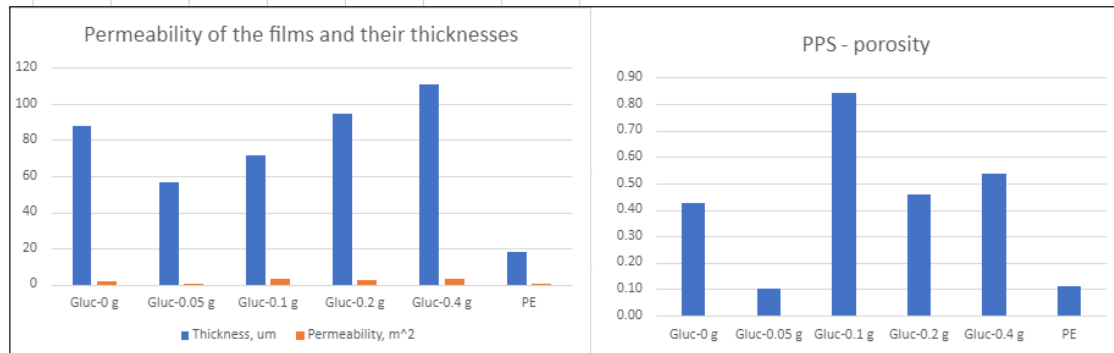


Figure 10: PPS-porosity and air permeability of the faceted films and PE film.

### 3.8 Transparency

The transparency of the faceted films was measured using SpectroScan Automated Scanner 36.62.11. Although faceting produced thick areas, but the films were transparent to some extent. The PE film transparency was 99.5% where the faceted film of 0.05 g surfactant gave a 75% transparency, as in Figure 11.

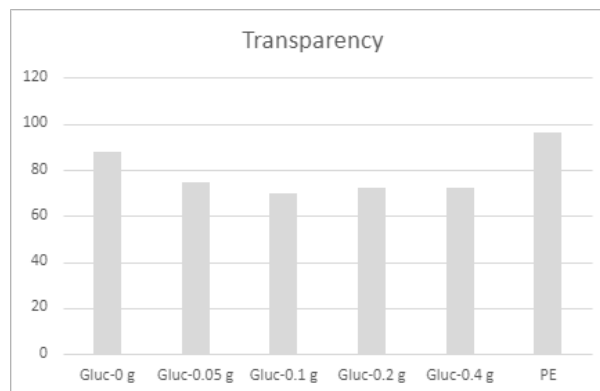
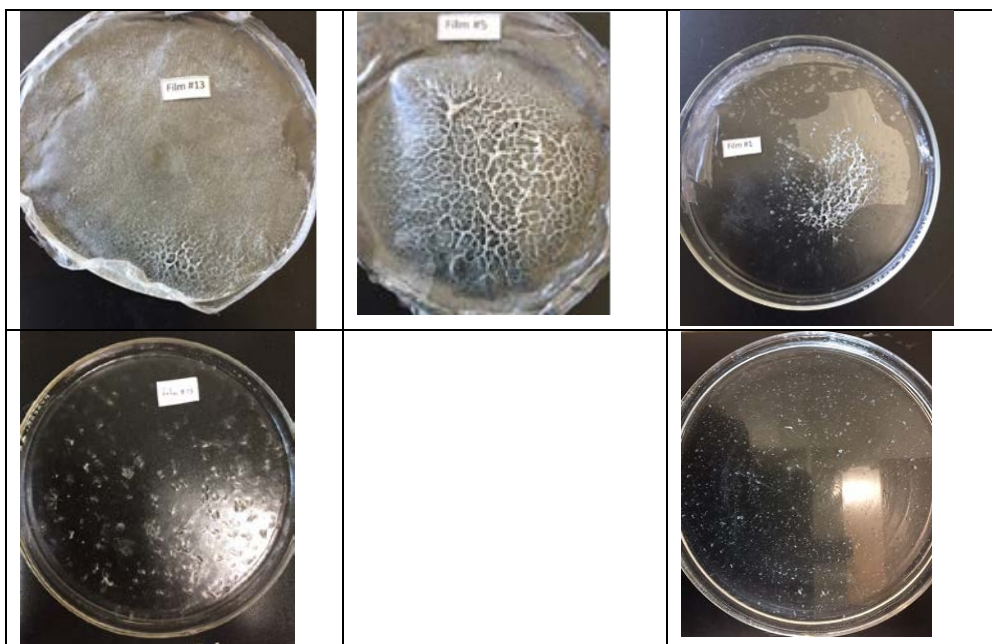


Figure 11: Transparency of glucomannan faceted films and PE film.

### 3.7 Faceting and phase transformation.

The dried films presented in Figure 12, exhibited a shape transformation, and solid polygons and fiber structures were formed. What happened at the glucomannan – water interface, is related to the surfactant freezing and depositing on the interface, due to a slow cooling rate and type of the surfactant (García-Aguilar *et al.*, 2021), (Wong *et al.*, 2019). These changes occurred at a temperature above the melting point of the polymer, where the interfacial monomer crystallizes (Guttman *et al.*, 2016). As the surfactant concentration increased, the surface tension of the glucomannan solution dropped and faceting began, all the films (1, 5, 13 and 15) showed faceting but in distinct shapes. Film 5 showed the highest deformed droplets, because it was dried a longer time over the weekend, but the trend shows that the films had faceted areas when the surfactants were at 40%, 20%, 10% and 5% concentration (from the top left clockwise).



*Figure 12: Glucomannan dried films, showing phase transformation at the polymer- water interface and a successful glucomannan film (last image to the right).*

The last image shows a successful film, formulated from the same ingredients as the Film 1; it required raising the reaction temperature up to 40°C and the drying conditions (57°C, 35% RH for 3 hours) followed by 18 hours at TAPPI testing conditions for paper. The film was clear and there were no faceting phenomena detected, it is ready for mechanical testing (Tensile strength, % elongation, roughness, caliper, and surface free energy) and water vapor and air permeability.

#### **4. Conclusion.**

The glucomannan is a promising biofilm for food packaging because it is originated from an annual plant and is friendly to the environment. Controlling the reaction temperature and cooling rate during drying is crucial in producing glucomannan films to use them in the packaging industry, printing, and printed electronics. The films should be clear, have good mechanical and barrier properties, smooth, transparent, and easy to print on. Selection of the appropriate surfactant and its concentration, as well as selecting proper mixing reaction temperature and drying conditions helps also in reducing the interfacial freezing effect and therefore producing the proper biofilms. The market of cellulose wrapping biofilms is worldwide and is a big one, however, the hemicellulose biofilms, like Glucomannan and Xylan, is still in its early stages.

## References

- Altay, B. N. *et al.* (2020) 'Surface Free Energy Estimation : A New Methodology for Solid Surfaces', 1901570, pp. 1–11. doi: 10.1002/admi.201901570.
- Chau, T. T. (2009) 'A review of techniques for measurement of contact angles and their applicability on mineral surfaces', *Minerals Engineering*, 22(3), pp. 213–219. doi: 10.1016/j.mineng.2008.07.009.
- Denkov, N. *et al.* (2015) 'Self-shaping of oil droplets via the formation of intermediate rotator phases upon cooling', *Nature*, 528(7582), pp. 392–395. doi: 10.1038/nature16189.
- García-Aguilar, I. *et al.* (2021) 'Faceting and Flattening of Emulsion Droplets: A Mechanical Model', *Physical Review Letters*, 126(3), p. 38001. doi: 10.1103/PhysRevLett.126.038001.
- Guttman, S. *et al.* (2016) 'How faceted liquid droplets grow tails', *Proceedings of the National Academy of Sciences of the United States of America*, 113(3), pp. 493–496. doi: 10.1073/pnas.1515614113.
- Honarvar, Z., Hadian, Z. and Mashayekh, M. (2016) 'Nanocomposites in food packaging applications and their risk assessment for health', *Electronic physician*, 8(6), pp. 2531–2538. doi: 10.19082/2531.
- Jonas, H. (2006) 'Hemicellulose as barrier material', (april), pp. 1–73.
- Kajiya, T. *et al.* (2009) 'Controlling the drying and film formation processes of polymer solution droplets with addition of small amount of surfactants', *Journal of Physical Chemistry B*, 113(47), pp. 15460–15466. doi: 10.1021/jp9077757.
- Kalia, S. *et al.* (2011) 'Cellulose-based bio- and nanocomposites: A review', *International Journal of Polymer Science*, 2011. doi: 10.1155/2011/837875.
- Lavoine, N., Desloges, I. and Bras, J. (2014) 'Microfibrillated cellulose coatings as new release systems for active packaging', *Carbohydrate Polymers*, 103(1), pp. 528–537. doi: 10.1016/j.carbpol.2013.12.035.
- Lee, H. V., Hamid, S. B. A. and Zain, S. K. (2014) 'Conversion of lignocellulosic biomass to nanocellulose: Structure and chemical process', *Scientific World Journal*, 2014(April). doi: 10.1155/2014/631013.
- Ma, R. (2018) 'Screen Printed Moisture Sensor On Barrier Coated SBS Board : The Characterizations of the Hemicellulose-Based Biofilms and Their Applications for Smart Packaging'.
- Ma, R., Pekarovicova, A. and Fleming, P. D. (2018) 'Biopolymer films from glucomannan: The effects of citric acid crosslinking on barrier properties', *Journal of Print and Media Technology Research*, 7(1), pp. 19–25. doi: 10.14622/JPMTR-1802.
- Makkonen, L. (2016) 'Young's equation revisited', *Journal of Physics Condensed Matter*, 28(13). doi: 10.1088/0953-8984/28/13/135001.
- Marin, O. *et al.* (2020) 'Polyhedral liquid droplets: Recent advances in elucidation and application', *Current Opinion in Colloid and Interface Science*, 49, pp. 107–117. doi: 10.1016/j.cocis.2020.05.006.
- Nair, S. B., Alummoottil N, J. and Moothandasserry S, S. (2017) 'Chitosan-konjac

glucomannan-cassava starch-nanosilver composite films with moisture resistant and antimicrobial properties for food-packaging applications', *Starch/Staerke*, 69(1–2). doi: 10.1002/star.201600210.

Nick Triantafillopoulos (1988) 'Measurement of Fluid Rheology and Interpretation of Rheograms by Measurement of Fluid Rheology and Interpretation of Rheograms Second Edition'. Available at: <http://www.kaltecsci.com/rheology.pdf>.

Owens, D. and Wendt, R. (1969) 'Estimation of the surface free energy of polymer', *Journal of Applied Polymer Science*, 13, pp. 1741–1747.

Pal, L., Joyce, M. K. and Fleming, P. D. (2006) 'A simple method for calculation of the permeability coefficient of porous media', *Tappi Journal*, 5(9), pp. 10–16.

Picout, D. R. and Ross-Murphy, S. B. (2003) 'Rheology of biopolymer solutions and gels.', *TheScientificWorldJournal*, 3, pp. 105–121. doi: 10.1100/tsw.2003.15.

*Rheological measurements* :: Anton Paar Wiki (no date). Available at: <https://wiki.anton-paar.com/en/basics-of-rheology/rheological-measurements/> (Accessed: 5 April 2021).

Rhim, J. W. and Ng, P. K. W. (2007) 'Natural biopolymer-based nanocomposite films for packaging applications', *Critical Reviews in Food Science and Nutrition*, 47(4), pp. 411–433. doi: 10.1080/10408390600846366.

Scheller, H. V. and Ulvskov, P. (2010) 'Hemicelluloses', *Annual Review of Plant Biology*, 61(1), pp. 263–289. doi: 10.1146/annurev-arplant-042809-112315.

Wang, K. *et al.* (2017) 'Structural characterization and properties of konjac glucomannan and zein blend films', *International Journal of Biological Macromolecules*, 105, pp. 1096–1104. doi: 10.1016/j.ijbiomac.2017.07.127.

Wong, C. K. *et al.* (2019) 'Faceted polymersomes: A sphere-to-polyhedron shape transformation', *Chemical Science*, 10(9), pp. 2725–2731. doi: 10.1039/c8sc04206c.